Canadian Science Publishing
NRC Research Press journals | Publishing Services

Biochemistry and Cell Biology
Biochimie et biologie cellulaire

Effect of pH on the structure, function and stability of human calcium/calmodulin-dependent protein kinase IV: A combined spectroscopic and MD simulation studies

Journal:	*Biochemistry and Cell Biology*
Manuscript ID	bcb-2015-0132.R1
Manuscript Type:	Article
Date Submitted by the Author:	30-Dec-2015
Complete List of Authors:	Naz, Huma; Jamia Millia Islamia, Centre for Interdisciplinary Research in Basic Sciences Shahbaaz, Mohd.; Durban University of Technology, Chemistry Bisetty, Krishna; Durban University of Technology, Chemistry Islam, Asimul; Jamia Millia Islamia, Centre for Interdisciplinary Research in Basic Sciences Ahmad, Faizan; Jamia Millia Islamia, Centre for Interdisciplinary Research in Basic Sciences Hassan, Imtaiyaz; Jamia Millia Islamia, Centre for Interdisciplinary Research in Basic Sciences
Keyword:	Calcium/calmodulin-dependent protein kinase IV, molecular dynamics simulation, kinase activity, spectroscopic techniques, effect of pH

Running Head: Effect of pH on CAMKIV

Effect of pH on the Structure, Function and Stability of Human Calcium/Calmodulin-Dependent Protein Kinase IV: A Combined Spectroscopic and MD Simulation Studies

Huma Naz[1], Mohd. Shahbaaz[2], Krishna Bisetty[2], Asimul Islam[1], Faizan Ahmad[1] and Md. Imtaiyaz Hassan[1,*]

[1]*Centre for Interdisciplinary Research in Basic Sciences, Jamia Millia Islamia, Jamia Nagar, New Delhi 110025, India.*

[2]*Department of Chemistry, Durban University of Technology, Durban-4000, South Africa*

***Correspondence:**

Md. Imtaiyaz Hassan, Ph.D.
Centre for Interdisciplinary Research in Basic Sciences,
Jamia Millia Islamia, Jamia Nagar,
New Delhi 110025, India
E-mail: mihassan@jmi.ac.in

Abstract

Human Calcium/calmodulin-dependent protein kinase IV (CAMKIV) is a member of Ser/Thr protein kinase family. It is regulated by the calcium-calmodulin dependent signal through a secondary messenger, Ca^{2+} that leads to the activation of its auto-inhibited form. The over-expression and mutation in CAMKIV as well as change in Ca^{2+} concentration is often associated with numerous neurodegenerative diseases and cancers. We have successfully cloned, expressed and purified functionally active kinase domain of human CAMKIV. To observe the effect of different pH conditions on the structural and functional properties of CAMKIV, we have used spectroscopic techniques such as circular diachroism (CD) and fluorescence. We have observed that within of the pH ranges from 5.0 - 11.5, the CAMKIV maintains its both secondary and tertiary structures along with its function, while significant aggregation was observed at acidic pH (2.0 to 4.5). We have also performed the ATPase activity assay in different pH conditions and found a significant correlation between structure and enzymatic activities of CAMKIV. *In silico* validations were further carried out by modeling the three-dimensional structure of CAMKIV and then subjected it to the molecular dynamics simulations in order to understand their conformational behavior in explicit water conditions. A strong correlation between spectroscopic observations and the outputs of molecular dynamics simulation was observed for the CAMKIV.

Keywords: Calcium/calmodulin-dependent protein kinase IV; molecular dynamics simulation; kinase activity; spectroscopic techniques; structure-function relationship; effect of pH

1. Introduction

Calcium-calmodulin dependent protein kinase IV (CAMKIV) is a multifunctional protein kinase belonging to the Ser/Thr kinase family (Tokumitsu et al. 1995). It is primarily involved in regulating calcium–signaling cascade associated with several essential cellular processes like apoptosis, cell signaling, osteoclast differentiation (Choi et al. 2013), cell proliferation (Ichinose et al. 2011) and ischemic tolerance (Soderling 1999). Unlike CaMKII, this kinase has restricted tissue distribution and is highly expressed in the nervous system cerebellum (Miyano 1992), hematopoietic system, whereas it is expressed comparatively at lower extent in spleen and the spermatids (Wu and Means 2000). A relatively high expression of CAMKIV in the neurons (Ohmstede and Bwl. Chem. 264 1989) clearly suggests that it has a direct involvement in neuronal communication via calcium mediating signaling (Hardingham and Bading 2010). This enzyme also plays an essential role in the neuroprotection by inhibiting the neuron degradation or apoptosis caused by caspases, a cell death protein CED3 (Ellis et al. 1991; See et al. 2001). CAMKIV also phosphorylates the histone deacetylase (HDAC4), resulting in neuroprotection in excitotoxic glutamate condition, a major cell death mechanism in cerebral ischemia (McCullough et al. 2013).

Extracellular factors such as peptide hormones, growth factors, neurotransmitters, and synaptic stimuli (Johannessen et al. 2004; Mayr and Montminy 2001; Shaywitz and Greenberg 1999) enhance the depolarization of the signal voltage gated channel which leads to increase concentration of calcium into the cytoplasm, and calcium binds to calmodulin, a calcium binding protein (Chatila et al. 1996). Furthermore, this binary complex binds to the auto-inhibited form of CAMKIV and accelerates its basal activity by releasing PP2A from its auto-inhibitory domain

(Means 2000). The catalytic activity of the enzyme was enhanced by another kinase CAMKK which phosphorylates Thr200 residue on its activation loop.

The activated form of CAMKIV phosphorylates the nuclear transcription factor cAMP response element-binding protein (CREB) at serine 133 (Sheng et al. 1991; Silva et al. 1998; Sun et al. 1994). The phosphorylated CREB interacts with the CREB-binding protein (CBP), which activates CRE (cAMP response element)-mediated transcription by the mobilization of CBP to the promoter regions of the target genes (Impey et al. 2002; Silva et al. 1998). CAMKIV regulates CREB–CBP-mediated transcription through their phosphorylation, acting as a key mediator of Ca^{+2} signal stimulated transcription activation. The mutation and over expression analyses showed that CAMKIV is directly associated with several life threatening diseases such as Alzheimer's disease (Loo et al. 1993), Huntington's disease (Portera-Cailliau et al. 1995), spinal muscular dystrophy (Roy et al. 1995), systemic lupus erythematosus (SLE) (Koga et al. 2012) and varieties of cancer such as lung carcinoma, hepatocellular carcinoma (Lin et al.) and epithelial ovarian cancer (Takai et al. 2002), as well as stroke (Liu et al.). Therefore, CAMKIV is considered as an important target for designing drug molecules of therapeutic applications (Hoda et al. 2015; Melnikova and Golden 2004).

CAMKIV is a 473-residue long polypeptide comprised of a 255-residue long protein kinase domain (46–300), a 17-residue long auto-inhibitory domain (305-321), a 13-residue long overlapping serine/threonine phosphatase 2A (PP2A)-binding domain (306-323) and a 20-residue long calmodulin-binding domain (322-341) (Kitani et al. 1994). Functions of other regions are still unknown. The auto-inhibitory domain overlaps with the calmodulin binding region and interacts in the inactive folded state with the catalytic domain as a pseudosubstrate

(Tokumitsu et al. 1994). CAMKIV has a general consensus phosphorylation sequence R-X-X-Ser/Thr motif, which is phosphorylated by the CaMKK and thus increases CAMKIV kinase activity significantly (Anderson and Kane 1998). Furthermore, binding of calmodulin to the CAMKIV results into a conformational change that relieves intrasteric autoinhibition and allows phosphorylation of Thr-200 within the activation loop by CaMKK1 or CaMKK2 (Hanissian et al. 1993; Krebs 1998). The phosphorylation of Thr-200 results into a 10-20-fold increase in total activity to generate Ca2+/calmodulin-independent activity. Autophosphorylation of the N-terminus Ser-12 and Ser-13 is required for full activation (Chow et al. 2005).

Despite of a well documented literature on the functional aspects of CAMKIV, a very little information is available on its biophysical properties (Naz et al. 2016; Naz et al. 2015b). It was observed that a change in Ca^{2+} concentration causes the lowering of extracellular pH, which disrupts the regulation of pH homeostasis, neuronal excitability and neuronal differentiation in brain as well (Obara et al. 2008; Sanchez-Armass et al. 2006). Besides, it also changes the protonation in glial cells leading to the glioma (McLean et al. 2000). To understand the effect of pH on the structure, function and stability of CAMKIV, we have cloned, expressed and purified human CAMKIV successfully from *E. coli* culture. We performed circular dichroism (CD) and fluorescence measurements at different pH values (2.0 to 11.0) to see the effect of pH on the secondary and tertiary structures, respectively. The structural features were further complemented by enzyme activity assay and molecular dynamics (MD) simulation studies to get a better insight into the structure-function relationship.

2. Materials and Methods

2.1. Materials

Media for bacterial culture Luria broth and Luria agar were purchased from Himedia. Agarose was purchased from Biobasic (Ontario, Canada). Restriction enzymes (*NdeI* and *XhoI*), PCR-*Taq* DNA polymerase, phusion polymerase and cloning-quick DNA ligase were purchased from Thermo Scientific (USA). Ampicillin, kanamycin, monoclonal anti-His antibody and DNA preparation kits were purchased from Sigma (St. Louis, MO). Ni-NTA column and gel filtration column Superdex-75 were purchased from GE healthcare (GE Healthcare Life Sciences, Uppsala, Sweden). All reagents for the buffer preparation are of analytical grade.

2.2. Cloning, expression and purification

Human *CAMK4* gene was purchased from DF/HCC DNA Resource Core, Harvard Medical School (http://plasmid.med.harvard.edu/PLASMID). The kinase domain of CAMKIV (residues 15-340) was amplified using forward primer with *NdeI* site: 5' AATCATATGTCTTCGGTCACCGCCAGTGCG 3' and reverse primer with *Xho1* site: 5' AATCTCGAGCAATCCCAGGCGGGAAGAGG 3'. The amplified gene was ligated into the pET28a(+) expression vector with 6His-tag at the N-terminus followed by the transformation into BL21 (DE3) strain of *E. coli.*

The transformed cells were grown in LB media at 37 °C up to the optical density of cells was reached to 0.6 at 600 nm. Culture was induced with 0.25 mM isopropyl β-D-1-thiogalactopyranoside, for four hours at 37 °C. The full grown culture was centrifuged at 6,000 rpm for 20 minutes at 4 °C, and pellet was dissolved in a buffer containing 50mM Tris, 20mM EDTA 0.1 mM PMSF and 1% of Triton 100 followed by the sonication for 20 min (10 sec off, 10 sec on). After the sonication, pellets were collected through centrifugation, and re-suspended in 50 mM Tris and 20 mM EDTA. Sonication and centrifugation were repeated twice. Pellets

were collected and washed with milliQ water thrice. Finally, inclusion bodies were dissolved in 1.0 ml of milliQ and stored at 4 °C.

The solubilisation of inclusion bodies was done in the lysis buffer (1.0% of N laurousyl sarcosine and 50 mM CAPS buffer pH 11.0) followed by centrifugation at 12,000 rpm for 20 minutes. Supernatant was loaded on to the Ni–NTA column which was equilibrated with the washing buffer (10 mM imidazole, 1.0% of N laurousyl sarcosine and 50 mM CAPS buffer pH 11.0). The bound protein was eluted with 400 mM imidazole concentration in the elution buffer (0.3% N-lauroyl sarcosine and 50 mM CAPS buffer pH 11.0). The purity of eluted fractions was checked by sodium dodecyl sulfate polyacrylamide gel electrophoresis (SDS–PAGE). Purified proteins were dialyzed for 48 hrs in 20 mM phosphate buffer + 100 mM NaCl, pH 7.4 with five successive changes to get the refolded protein. The concentration of the dialyzed and stock solutions of CAMKIV was determined experimentally using molar absorption coefficient value of 47245 M^{-1} cm^{-1} at 280 nm (Edelhoch 1967; Pace et al. 1995).

2.3. Sample preparation

The pH based structure analyses were done using different buffers having broad pH ranges from 2.0 to 11.5. To prepare buffers of pH values 2.0, 2.5. 3.0 and 3.5, 50 mM glycine solution was used and pH was adjusted using HCl. For buffers of pH values 4.0, 4.5, 5.0 and 5.5, 50 mM acetate-50mM citrate solution was used and pH was adjusted using acetic acid and citric acid. Buffers of pH values 6.0, 6.5 and 7.0 were prepared by using 50 mM MES. For pH values of 7.5, 8.0, 8.5 and 9.0, 50 mM Tris buffer was used (pH adjusted using HCl). For preparing buffers of pH values 9.5 and 10.0 sodium bicarbonate buffer was used and pH was adjusted by $NaHCO_3$. To prepare buffers of pH values 10.0, 10.5 11.0 and 11.5 50 mM glycine solution was used and

pH was adjusted using NaOH. CAMKIV was incubated in the different buffers for 4 hrs at 25°C before the spectroscopic measurements. This incubation time was sufficient to attain equilibrium.

2.4. CD measurements

Secondary structure of CAMKIV was measured in Jasco spectropolarimeter (J-1500), equipped with a peltier for temperature control (PTC-348WI). For the far-UV CD measurements 0.24 mg/ml of CAMKIV was used. Spectra were collected in the range of 200-250 nm (25 ± 0.1 °C). Each spectrum was obtained by averaging five to eight successive accumulations with a wavelength step of 0.2 nm at a rate of 100 nm min−1, response time 1 s, and band width 1 nm. Results of CD measurements were expressed as mean residue ellipticity ($[\theta]_\lambda$) in deg cm^2 $dmol^{-1}$ at a given wavelength, λ (nm) using the relation,

Mean residue ellipticity $[\theta]_\lambda = M_0\theta/10.l.c$ (1)

where M_0 is the mean residue weight of the protein, θ_λ is the observed ellipticity in milli degrees at λ, l is the path length of the cell in centimeters, and c is the protein concentration in mg ml^{-1}. The observed $[\theta]_\lambda$ of the protein was corrected for the contribution of the solvent (Kelly et al. 2005). All CD measurements were done at least three times at each pH.

2.5. Measurements of fluorescence spectra

Fluorescence spectra of CAMKIV were measured in Jasco fluorimeter (FP-6200) in a quartz cuvete of path length 3 mm at 25 ± 0.1 °C. The temperature was maintained by an external thermostated water circulator. Both excitation and emission slits were set at 5 nm. For the

fluorescence measurements, the excitation wavelength was set at 292 nm, and Trp-emission spectra were acquired in the wavelength range of 300-400 nm. Protein concentration used was 0.24 mg/ml. The value of blank solution was subtracted from the value of each sample. All measurements were done at least three times at each pH.

2.6. Measurements of absorption spectra

Absorption spectra of human CAMKIV was measured in Shimadzu 1601 UV/Vis spectrophotometer connected with a temperature controlling external water bath. All measurements were carried out using 1 cm path length cuvette in the wavelength range 240–340 nm at a protein concentration of 0.1 mg/ml. All spectral measurements were done at least three times at each pH.

2.7. ATPase assay

We have performed the ATPase assay for CAMKIV at different pH values in triplicate. The hydrolysis of ATP catalyzed by CAMKIV was assayed by measuring the formation of ^{32}P from [γ-^{32}P] ATP. The reaction was performed for 2 h at 37 °C in the presence of enzyme and a mixture of [γ-^{32}P] ATP (specific activity 222 TBq $mmol^{-1}$) and cold ATP (1 mM). Protein concentration for activity measurement was 200 ng.

2.8. MD simulations

The protein were subjected to molecular dynamics (MD) simulations by using GROMACS (Pronk et al. 2013) package at different pH conditions (version 4.6.5, installed on the CHPC server which provides 15 nodes with 8 cores per node of space for computation). Different pH

environments were created for 4-amino (sulfamoyl-phenylamino)-triazole-carbothioic acid by altering the protonation state of titration sites. We predicted these titrable residues in the structure of the respective protein by using "Prepare protein" module of Discover Studio 4.0 (BIOVIA 2013). We perform the protonation and deprotonation of the titrable groups using their known pKa values. The topologies of the protein at different pH conditions were generated using CHARMM 36 force field (Huang and MacKerell 2013). The SPC/E water model (Zielkiewicz 2005) was used at different pH conditions for the solvation of the protein, and by using steepest descent algorithm we perform the energy minimization with a convergence criterion of 0.005 kcal mol^{-1}.

The equilibration phase was carried out under constant volume (NVT) and constant pressure (NPT) ensemble conditions. The temperature of system was maintained at 300 K by using Berendsen weak coupling method in both ensemble conditions along with pressure which was maintained at 1 bar by utilizing Parrinello-Rahman barostat in constant pressure ensemble. Finally, MD production was carried by using LINCS algorithm for each complex at 20 ns time scale. The knowledge extracted from the trajectory files was utilized for understanding the behavior of protein in the explicit water environment with different pH conditions. Root mean square deviations (RMSD), radius of gyration (*R*g) and root mean square fluctuations (RMSF) were analyzed.

3. Results & Discussion

CAMKIV has wide range of tissue expression especially in the brain (Bland et al. 1994), thymus (Jang et al. 2001), neuronal subpopulations (Ohmstede and Bwl. Chem. 264 1989), spleen and testis (Wu et al. 2000). This protein is playing critically important role in the cell proliferation,

gene expression, apoptosis, muscle contraction and neurotransmitter release (Bachs et al. 1992; Bito et al. 1997; Lu and Hunter 1995; Nicotera et al. 1994). The regulation of CAMKIV is a tightly controlled process (Anderson et al. 2004; Hanissian et al. 1993), and involves several steps. In all these processes the environmental condition such as ionic strength and pH plays a critical role. Hence, we performed pH dependent studies on CAMKIV for understanding the effect of pH on the structure, stability and thus function.

3.1. Far-UV CD measurements

Far-UV CD spectra (200 nm to 250 nm) of CAMKIV were collected to see the effect of pH on its secondary structure. CD spectrum of the native CAMKIV shows characteristic double minima at 208 and 222 nm **(Figure 1).** CAMKIV belongs to the α/β class of proteins, and the secondary structure content determined from the crystal structure consists of 31% α-helix (13 helices; 110 residues) and 13% β-structure (10 strands; 46 residues) (Protein Data Bank Code: 2W4O). We have analysed the CD spectra of the native protein (Figure 1) for estimating α-helical and β-structure contents as a function of pH using the Dichroweb K2D server (Perez-Iratxeta and Andrade-Navarro 2008), which are listed in Table 1. In the native pH conditions (pH 6.5 - 7.5), helical content is about 29±2% and β-structure is 16±2%, which is in excellent agreement with those derived from the crystal structure data.

The far-UV CD spectra in basic pH range (pH 7.5-11.5) are almost identical **(Figure 1A)**. However, in the acidic conditions, the far-UV CD spectra show distinct differences between alkaline and acidic pH values **(Figure 1B)**. If we increase pH from 7.0 to 11.5 there is no significant differences among spectra suggesting that CAMKIV maintains its secondary structure in the alkaline pH range. On the other hand, if we move towards the acidic side, the far-UV CD

spectra are not significantly different till the pH 5.5. On further decreasing the pH a remarkable decrease in the dichroic signal was observed. The CD signal was completely disappeared at pH 2.0 (Figure 1B). All these observations clearly indicate that CAMKIV maintains its secondary structure in the pH range of 5.5 to 11.5. At acidic pH CAMKIV is aggregating and hence it may not be functionally active.

3.2. Fluorescence measurements

After secondary structure analysis we tried to see the effect of pH on the tertiary structure of CAMKIV by monitoring change in the environment of the aromatic amino acid residues. Since, the change in intrinsic fluorescence is an indication for change aromatic amino acid residues in CAMKIV. Therefore, tryptophan intrinsic fluorescence was monitored by measuring emission spectra from 300 to 400 nm, with excitation at 290 nm. **Figure 2A** shows the fluorescence emission spectra of CAMKIV in the pH range of 7.5 to 11.5. No significant change was observed for the peak of fluorescence maxima, indicating that tryptophan environment in this pH range does not get disturbed significantly. However, a considerable decrease in fluorescence intensity was observed. This decrease in the fluorescence intensity could be due to deprotonation of neighboring basic amino acids. These observations suggest that the tertiary structure of CAMKIV remains unchanged in the alkaline pH range.

Figure 2B shows the fluorescence emission spectra of CAMKIV in the pH range of 7.0-2.0. A marked blue shift in the intrinsic fluorescence spectra was induced by the pH drop. The greatest differences were between pH 7.0 and 2.0 with as much as 9 nm wavelength differ. Shifting of the peak at acidic pH range may occurred be due to disruption of electrostatic interaction and the ionization of tryptophan which could be the cause of conformational changes (Yang and Honig

1995). We got a visible aggregation at pH values 3.0, 3.5, 4.5 and 5.0. Hence, the data of these pHs are not included in the figure. Our results suggest conformational changes at lover acidic pH values. This finding is in agreement with that of CD measurements which showed that CAMKIV is acid denatured at lower pH values. All these findings shed light onto the effect of the complete protonation/deprotonation of all amino acid side groups which likely led to the disruption of internal salt bridges, and other non-covalent interactions (Yang and Honig 1995).

3.3. Absorption measurements

The effect of pH on the tertiary structure of CAMKIV was further examined by absorption spectra measurements (240-340 nm). In the basic pH range (7.5 to 11.5) a decrease in absorption was observed without any shifting of absorption maxima **(Figure 3A)**. The direction of Trp peak shifts is usually highly sensitive to the microenvironment of each residue, with blue shifts in UV spectra and red shifts in fluorescence spectra generally indicating increased solvent exposure (Hospes et al. 2013). Hence, there is no any significant change was observed while increasing the pH of CAMKIV from 7.5 to 11.5. On the other hand, a remarkable changes in the absorption spectra of CAMKIV was observed on decreasing the pH from 7.0 to 2.0 (Figure 3B). The UV absorption spectra in the alkaline region is opposite to the acidic condition, yet consistent trend relative to the fluorescence data, with a considerable blue shifts shown in Figure 2B indicating that the Trp residues have become more solvent accessible.

3.4. Activity assay

To observe the effect of pH on the function of CAMKIV, we have performed enzyme activity assay. CAMKIV has the ability to catalyze the hydrolysis of ATP and the formation of ^{32}P from [γ-^{32}P] ATP which were assayed radiographically (Naz et al. 2015a). **Figure 4** shows that

CAMKIV catalyzes the hydrolysis of ATP in the alkaline pH range. However, a remarkable decrease in the CAMKIV activity was observed as we lower down the pH from 7.0 to 2.0. These observations further validate the structural changes with reference to the pH of the system.

3.5. MD simulations

MD simulation in combinations with experimental studies help to get better insight into the conformation of protein in different environments (Anwer et al. 2015; Idrees et al. 2015; Khan et al. 2016a; Khan et al. 2016b; Khan et al. 2016c; Naiyer et al. 2015; Ubaid-Ullah et al. 2014). After equilibration CAMKIV was simulated for 20 ns at different protonation state, its behavior is analyzed using the utilities of GROMACS. 4-Amino(sulfamoyl-phenylamino)-triazole-carbothioic acid showed relatively higher value for average RMSD in pH range from 2 to 5, indicative of its instability in the acidic conditions. The titration results showed that the relative folding energy of the protein was comparatively low in the pH range of 6.0-10.0 (**Figure 5**), which is indicative of the stability of the protein in these particular range. The differentially protonated protein was immersed in the SPC/E water model and minimized in the 1800 steps of steepest descent.

At pH 2.0, the average RMSD value was found to be 0.55 nm, while for pH values in the range 3.0-5.0 it showed an increment with 1.09 nm at pH 3.0, 0.82 at pH 4.0 while at pH 5.0 it was calculated to be 0.66 nm. These values are comparatively higher than the rest of the pH conditions (**Figure 6A**), which is an indicative of the wider range stability of CAMKIV. While the lowest RMSD values of 0.41nm, 0.45 nm and 0.46 nm were observed at pH 6.0, pH 10.0 and pH 11.0, respectively. The RMSD values for atoms of all the structures were

calculated by aligning all frames to initial structure using the mass-weighted least-squares fitting method.

Similarly, the *R*g plots also showed a similar behavior as higher fluctuations were observed at the acidic pH (2.0-5.0), as compared to the pH ranges from 6.0 to 12.0 (**Figure 6B**). The average *R*g values from pH 2-5 were found to be 2.20 nm, 2.31 nm, 2.20 nm and 2.23 nm, respectively. While for pH 6.0, 10.0 and 11.0 least fluctuations were observed (**Figure 6B**); with average *R*g values were calculated to be 2.13 nm, 2.19 nm and 2.12 nm, respectively. These results were complemented by the RMSF plot which showed higher residual fluctuations at the acidic pH as compared to the rest of the conditions (**Figure 7**). A consistent correlation was observed for both spectroscopic and MD simulation data.

Conclusions

Here we described cloning, expression and purification of CAMKIV protein which was expressed in high yield and refolded successfully to have significant structure and essential enzyme activity. The secondary and tertiary structures of CAMKIV were measured at different pH ranges. We found that this protein maintains both secondary and tertiary structure in the alkaline pH range. However, a remarkable effect of pH on the structure and stability of CAMKIV was observed in the acidic pH range. A close correlation was also observed during the MD simulation studies. pH dependent structural studies followed by MD simulations and biochemical assays will be helpful for better understanding of the dynamic behavior of the CAMKIV and its function in different organelle and regulation of cellular physiology. Furthermore, our study has demonstrated that structural property of the

CAMKIV is dependent on the pH of the medium which may provides a molecular basis for understanding of its function in the different conditions.

Acknowledgements

MIH and HN are thankful the Indian Council of Medical Research, Government of India for financial assistance. We sincerely thank Jamia Millia Islamia and Durban University of Technology for providing high speed computing facilities. Authors sincerely thank to the Department of Science and Technology, Government of India for the FIST support (FIST program No. SR/FST/LSI-541/2012).

Conflict of Interest

The authors have no substantial financial or commercial conflicts of interest with the current work or its publication.

References

Anderson, K.A., and Kane, C.D. 1998. Ca2+/calmodulin-dependent protein kinase IV and calcium signaling. Biometals **11** (4): 331-343.

Anderson, K.A., Noeldner, P.K., Reece, K., Wadzinski, B.E., and Means, A.R. 2004. Regulation and function of the calcium/calmodulin-dependent protein kinase IV/protein serine/threonine phosphatase 2A signaling complex. J Biol Chem **279** (30): 31708-31716. 10.1074/jbc.M404523200
M404523200 [pii].

Anwer, K., Sonani, R., Madamwar, D., Singh, P., Khan, F., Bisetty, K., Ahmad, F., and Hassan, M.I. 2015. Role of N-terminal residues on folding and stability of C-phycoerythrin: simulation and urea-induced denaturation studies. Journal of Biomolecular Structure and Dynamics **33** (1): 121-133.

Bachs, O., Agell, N., and Carafoli, E. 1992. Calcium and calmodulin function in the cell nucleus. Biochim Biophys Acta **1113** (2): 259-270.

BIOVIA, D.S. (2013). Discovery Studio Modeling Environment (San Diego: Dassault Systèmes).

Bito, H., Deisseroth, K., and Tsien, R.W. 1997. Ca2+-dependent regulation in neuronal gene expression. Curr Opin Neurobiol **7** (3): 419-429. S0959-4388(97)80072-4 [pii].

Bland, M.M., Monroe, R.S., and Ohmstede, C.A. 1994. The cDNA sequence and characterization of the Ca2+/calmodulin-dependent protein kinase-Gr from human brain and thymus. Gene **142** (2): 191-197.

Chatila, T., Anderson, K.A., Ho, N., and Means, A.R. 1996. A unique phosphorylation-dependent mechanism for the activation of Ca2+/calmodulin-dependent protein kinase type IV/GR. J Biol Chem **271** (35): 21542-21548.

Choi, Y.H., Ann, E.J., Yoon, J.H., Mo, J.S., Kim, M.Y., and Park, H.S. 2013. Calcium/calmodulin-dependent protein kinase IV (CaMKIV) enhances osteoclast differentiation via the up-regulation of Notch1 protein stability. Biochim Biophys Acta **1833** (1): 69-79. 10.1016/j.bbamcr.2012.10.018
S0167-4889(12)00300-X [pii].

Chow, F.A., Anderson, K.A., Noeldner, P.K., and Means, A.R. 2005. The autonomous activity of calcium/calmodulin-dependent protein kinase IV is required for its role in transcription. J Biol Chem **280** (21): 20530-20538. M500067200 [pii]
10.1074/jbc.M500067200.

Edelhoch, H. 1967. Spectroscopic determination of tryptophan and tyrosine in proteins. Biochemistry **6** (7): 1948-1954.

Ellis, R.E., Yuan, J.Y., and Horvitz, H.R. 1991. Mechanisms and functions of cell death. Annu Rev Cell Biol **7** 663-698. 10.1146/annurev.cb.07.110191.003311.

Hanissian, S.H., Frangakis, M., Bland, M.M., Jawahar, S., and Chatila, T.A. 1993. Expression of a Ca2+/calmodulin-dependent protein kinase, CaM kinase-Gr, in human T lymphocytes. Regulation of kinase activity by T cell receptor signaling. J Biol Chem **268** (27): 20055-20063.

Hardingham, G.E., and Bading, H. 2010. Synaptic versus extrasynaptic NMDA receptor signalling: implications for neurodegenerative disorders. Nat Rev Neurosci **11** (10): 682-696. 10.1038/nrn2911
nrn2911 [pii].

Hoda, N., Naz, H., Jameel, E., Shandilya, A., Dey, S., Hassan, M.I., Ahmad, F., and Jayaram, B. 2015. Curcumin specifically binds to the human calcium-calmodulin-dependent protein kinase IV: fluorescence and molecular dynamics simulation studies. J Biomol Struct Dyn 1-13. 10.1080/07391102.2015.1046934.

Hospes, M., Hendriks, J., and Hellingwerf, K.J. 2013. Tryptophan fluorescence as a reporter for structural changes in photoactive yellow protein elicited by photo-activation. Photochem Photobiol Sci **12** (3): 479-488. 10.1039/c2pp25222h.

Huang, J., and MacKerell, A.D., Jr. 2013. CHARMM36 all-atom additive protein force field: validation based on comparison to NMR data. J Comput Chem **34** (25): 2135-2145. 10.1002/jcc.23354.

Ichinose, K., Rauen, T., Juang, Y.T., Kis-Toth, K., Mizui, M., Koga, T., and Tsokos, G.C. 2011. Cutting edge: Calcium/Calmodulin-dependent protein kinase type IV is essential for mesangial cell proliferation and lupus nephritis. J Immunol **187** (11): 5500-5504. 10.4049/jimmunol.1102357
jimmunol.1102357 [pii].

Idrees, D., Prakash, A., Haque, M.A., Islam, A., Ahmad, F., and Hassan, M.I. 2015. Spectroscopic and MD simulation studies on unfolding processes of mitochondrial carbonic anhydrase VA induced by urea. J Biomol Struct Dyn 1-37. 10.1080/07391102.2015.1100552.

Impey, S., Fong, A.L., Wang, Y., Cardinaux, J.R., Fass, D.M., Obrietan, K., Wayman, G.A., Storm, D.R., Soderling, T.R., and Goodman, R.H. 2002. Phosphorylation of CBP mediates transcriptional activation by neural activity and CaM kinase IV. Neuron **34** (2): 235-244. S0896627302006542 [pii].

Jang, M.K., Goo, Y.H., Sohn, Y.C., Kim, Y.S., Lee, S.K., Kang, H., Cheong, J., and Lee, J.W. 2001. Ca2+/calmodulin-dependent protein kinase IV stimulates nuclear factor-kappa B transactivation via phosphorylation of the p65 subunit. J Biol Chem **276** (23): 20005-20010. 10.1074/jbc.M010211200
M010211200 [pii].

Johannessen, M., Delghandi, M.P., and Moens, U. 2004. What turns CREB on? Cell Signal **16** (11): 1211-1227. 10.1016/j.cellsig.2004.05.001
S0898656804000804 [pii].

Kelly, S.M., Jess, T.J., and Price, N.C. 2005. How to study proteins by circular dichroism. Biochim Biophys Acta **1751** (2): 119-139. S1570-9639(05)00179-2 [pii]
10.1016/j.bbapap.2005.06.005.

Khan, F.I., Aamir, M., Wei, D.Q., Ahmad, F., and Hassan, M.I. 2016a. Molecular mechanism of Ras-related protein Rab-5A and effect of mutations in the catalytically active phosphate-binding loop. J Biomol Struct Dyn 1-36. 10.1080/07391102.2015.1134346.

Khan, F.I., Shahbaaz, M., Bisetty, K., Waheed, A., Sly, W.S., Ahmad, F., and Hassan, M.I. 2016b. Large scale analysis of the mutational landscape in beta-glucuronidase: A major player of mucopolysaccharidosis type VII. Gene **576** (1 Pt 1): 36-44. 10.1016/j.gene.2015.09.062
S0378-1119(15)01171-3 [pii].

Khan, P., Parkash, A., Islam, A., Ahmad, F., and Hassan, M.I. 2016c. Molecular basis of the structural stability of hemochromatosis factor E: A combined molecular dynamic simulation and GdmCl-induced denaturation study. Biopolymers **105** (3): 133-142. 10.1002/bip.22760.

Kitani, T., Okuno, S., and Fujisawa, H. 1994. cDNA cloning and expression of human calmodulin-dependent protein kinase IV. J Biochem **115** (4): 637-640.

Koga, T., Ichinose, K., Mizui, M., Crispin, J.C., and Tsokos, G.C. 2012. Calcium/calmodulin-dependent protein kinase IV suppresses IL-2 production and regulatory T cell activity in lupus. J Immunol **189** (7): 3490-3496. jimmunol.1201785 [pii]
10.4049/jimmunol.1201785.

Krebs, J. 1998. Calmodulin-dependent protein kinase IV: regulation of function and expression. Biochim Biophys Acta **1448** (2): 183-189. S0167-4889(98)00142-6 [pii].

Lin, F., Marcelo, K.L., Rajapakshe, K., Coarfa, C., Dean, A., Wilganowski, N., Robinson, H., Sevick, E., Bissig, K.D., Goldie, L.C., *et al.* The camKK2/camKIV relay is an essential regulator of hepatic cancer. Hepatology **62** (2): 505-520. 10.1002/hep.27832.

Liu, L., McCullough, L., and Li, J. Genetic deletion of calcium/calmodulin-dependent protein kinase kinase beta (CaMKK beta) or CaMK IV exacerbates stroke outcomes in ovariectomized (OVXed) female mice. BMC Neurosci **15** 118. s12868-014-0118-2 [pii]
10.1186/s12868-014-0118-2.

Loo, D.T., Copani, A., Pike, C.J., Whittemore, E.R., Walencewicz, A.J., and Cotman, C.W. 1993. Apoptosis is induced by beta-amyloid in cultured central nervous system neurons. Proc Natl Acad Sci U S A **90** (17): 7951-7955.

Lu, K.P., and Hunter, T. 1995. The NIMA kinase: a mitotic regulator in Aspergillus nidulans and vertebrate cells. Prog Cell Cycle Res **1** 187-205.

Mayr, B., and Montminy, M. 2001. Transcriptional regulation by the phosphorylation-dependent factor CREB. Nat Rev Mol Cell Biol **2** (8): 599-609. 10.1038/35085068
35085068 [pii].

McCullough, L.D., Tarabishy, S., Liu, L., Benashski, S., Xu, Y., Ribar, T., Means, A., and Li, J. 2013. Inhibition of calcium/calmodulin-dependent protein kinase kinase beta and calcium/calmodulin-dependent protein kinase IV is detrimental in cerebral ischemia. Stroke **44** (9): 2559-2566. 10.1161/STROKEAHA.113.001030
STROKEAHA.113.001030 [pii].

McLean, L.A., Roscoe, J., Jorgensen, N.K., Gorin, F.A., and Cala, P.M. 2000. Malignant gliomas display altered pH regulation by NHE1 compared with nontransformed astrocytes. Am J Physiol Cell Physiol **278** (4): C676-688.

Means, A.R. 2000. Regulatory cascades involving calmodulin-dependent protein kinases. Mol Endocrinol **14** (1): 4-13. 10.1210/mend.14.1.0414.

Melnikova, I., and Golden, J. 2004. Targeting protein kinases. Nat Rev Drug Discov **3** (12): 993-994. 10.1038/nrd1600.

Miyano, O., Kameshita, I., and Fujisawa, H. (1992) J. Bid. Chem. 267, 1198-1203 1992. Purification and Characterization of Brain-specific Multifunctional
Calmodulin-dependent Protein Kinase from Rat Cerebellum. J Biol Chem **267** (January 15): 1198-1203.

Naiyer, A., Hassan, M.I., Islam, A., Sundd, M., and Ahmad, F. 2015. Structural characterization of MG and pre-MG states of proteins by MD simulations, NMR, and other techniques. Journal of Biomolecular Structure and Dynamics (ahead-of-print): 1-18.

Naz, F., Singh, P., Islam, A., Ahmad, F., and Imtaiyaz Hassan, M. 2015a. Human microtubule affinity-regulating kinase 4 is stable at extremes of pH. Journal of Biomolecular Structure and Dynamics 1-11.

Naz, H., Islam, A., Ahmad, F., and Hassan, M.I. 2016. Calcium/Calmodulin-dependent protein kinase IV: A multifunctional enzyme and potential therapeutic target. Progress in Biophysics and Molecular Biology.

Naz, H., Jameel, E., Hoda, N., Shandilya, A., Khan, P., Islam, A., Ahmad, F., Jayaram, B., and Hassan, M.I. 2015b. Structure guided design of potential inhibitors of human calcium-calmodulin dependent protein kinase IV containing pyrimidine scaffold. Bioorganic & Medicinal Chemistry Letters.

Nicotera, P., Zhivotovsky, B., and Orrenius, S. 1994. Nuclear calcium transport and the role of calcium in apoptosis. Cell Calcium **16** (4): 279-288. 0143-4160(94)90091-4 [pii].

Obara, M., Szeliga, M., and Albrecht, J. 2008. Regulation of pH in the mammalian central nervous system under normal and pathological conditions: facts and hypotheses. Neurochem Int **52** (6): 905-919. S0197-0186(07)00302-6 [pii]
10.1016/j.neuint.2007.10.015.

Ohmstede, C.-A., Jensen, K. F., and Sahyoun, N. E. (1989) J., and Bwl. Chem. 264, -. 1989. Ca2+/calmodulin-dependent protein kinase enriched in cerebellar granule cells. Identification of a novel neuronal calmodulin-dependent protein kinase. J Biol Chem **264** (April 5): 5866-5875.

Pace, C.N., Vajdos, F., Fee, L., Grimsley, G., and Gray, T. 1995. How to measure and predict the molar absorption coefficient of a protein. Protein Sci **4** (11): 2411-2423. 10.1002/pro.5560041120.

Perez-Iratxeta, C., and Andrade-Navarro, M.A. 2008. K2D2: estimation of protein secondary structure from circular dichroism spectra. BMC Struct Biol **8** 25. 10.1186/1472-6807-8-25
1472-6807-8-25 [pii].

Portera-Cailliau, C., Hedreen, J.C., Price, D.L., and Koliatsos, V.E. 1995. Evidence for apoptotic cell death in Huntington disease and excitotoxic animal models. J Neurosci **15** (5 Pt 2): 3775-3787.

Pronk, S., Pall, S., Schulz, R., Larsson, P., Bjelkmar, P., Apostolov, R., Shirts, M.R., Smith, J.C., Kasson, P.M., van der Spoel, D.*, et al.* 2013. GROMACS 4.5: a high-throughput and highly parallel open source molecular simulation toolkit. Bioinformatics **29** (7): 845-854. 10.1093/bioinformatics/btt055
btt055 [pii].

Roy, N., Mahadevan, M.S., McLean, M., Shutler, G., Yaraghi, Z., Farahani, R., Baird, S., Besner-Johnston, A., Lefebvre, C., Kang, X., *et al.* 1995. The gene for neuronal apoptosis inhibitory protein is partially deleted in individuals with spinal muscular atrophy. Cell **80** (1): 167-178. 0092-8674(95)90461-1 [pii].

Sanchez-Armass, S., Sennoune, S.R., Maiti, D., Ortega, F., and Martinez-Zaguilan, R. 2006. Spectral imaging microscopy demonstrates cytoplasmic pH oscillations in glial cells. Am J Physiol Cell Physiol **290** (2): C524-538. 00290.2005 [pii] 10.1152/ajpcell.00290.2005.

See, V., Boutillier, A.L., Bito, H., and Loeffler, J.P. 2001. Calcium/calmodulin-dependent protein kinase type IV (CaMKIV) inhibits apoptosis induced by potassium deprivation in cerebellar granule neurons. FASEB J **15** (1): 134-144. 10.1096/fj.00-0106com 15/1/134 [pii].

Shaywitz, A.J., and Greenberg, M.E. 1999. CREB: a stimulus-induced transcription factor activated by a diverse array of extracellular signals. Annu Rev Biochem **68** 821-861. 10.1146/annurev.biochem.68.1.821.

Sheng, M., Thompson, M.A., and Greenberg, M.E. 1991. CREB: a Ca(2+)-regulated transcription factor phosphorylated by calmodulin-dependent kinases. Science **252** (5011): 1427-1430.

Silva, A.J., Kogan, J.H., Frankland, P.W., and Kida, S. 1998. CREB and memory. Annu Rev Neurosci **21** 127-148. 10.1146/annurev.neuro.21.1.127.

Soderling, T.R. 1999. The Ca-calmodulin-dependent protein kinase cascade. Trends Biochem Sci **24** (6): 232-236. S0968000499013833 [pii].

Sun, P., Enslen, H., Myung, P.S., and Maurer, R.A. 1994. Differential activation of CREB by Ca2+/calmodulin-dependent protein kinases type II and type IV involves phosphorylation of a site that negatively regulates activity. Genes Dev **8** (21): 2527-2539.

Takai, N., Miyazaki, T., Nishida, M., Nasu, K., and Miyakawa, I. 2002. Ca(2+)/calmodulin-dependent protein kinase IV expression in epithelial ovarian cancer. Cancer Lett **183** (2): 185-193. S0304383502001076 [pii].

Tokumitsu, H., Brickey, D.A., Glod, J., Hidaka, H., Sikela, J., and Soderling, T.R. 1994. Activation mechanisms for Ca2+/calmodulin-dependent protein kinase IV. Identification of a brain CaM-kinase IV kinase. J Biol Chem **269** (46): 28640-28647.

Tokumitsu, H., Enslen, H., and Soderling, T.R. 1995. Characterization of a Ca2+/calmodulin-dependent protein kinase cascade. Molecular cloning and expression of calcium/calmodulin-dependent protein kinase kinase. J Biol Chem **270** (33): 19320-19324.

Ubaid-Ullah, S., Haque, M.A., Zaidi, S., Hassan, M.I., Islam, A., Batra, J.K., Singh, T.P., and Ahmad, F. 2014. Effect of sequential deletion of extra N-terminal residues on the structure and

stability of yeast iso-1-cytochrome-c. J Biomol Struct Dyn **32** (12): 2005-2016. 10.1080/07391102.2013.848826.

Wu, J.Y., and Means, A.R. 2000. Ca(2+)/calmodulin-dependent protein kinase IV is expressed in spermatids and targeted to chromatin and the nuclear matrix. J Biol Chem **275** (11): 7994-7999.

Wu, J.Y., Ribar, T.J., Cummings, D.E., Burton, K.A., McKnight, G.S., and Means, A.R. 2000. Spermiogenesis and exchange of basic nuclear proteins are impaired in male germ cells lacking Camk4. Nat Genet **25** (4): 448-452. 10.1038/78153.

Yang, A.S., and Honig, B. 1995. Free energy determinants of secondary structure formation: II. Antiparallel beta-sheets. J Mol Biol **252** (3): 366-376. S0022-2836(85)70503-7 [pii] 10.1006/jmbi.1995.0503.

Zielkiewicz, J. 2005. Structural properties of water: comparison of the SPC, SPCE, TIP4P, and TIP5P models of water. J Chem Phys **123** (10): 104501. 10.1063/1.2018637.

Figure Legends

Figure 1: Far UV CD spectra of CAMKIV in the pH ranges from 7.0 - 11.5 **(A),** and from7.5 to 2.0 **(B)**.

Figure 2: Fluorescence emission spectra of CAMKIV in the pH ranges from 7.0 to 11.5**(A)**, and from 7.5 to 2.0 **(B)**. Protein was excited at 292 nm and emission spectra were collected in the range of 300-400 nm.

Figure 3: Absorbance spectra of CAMKIV in pH ranges from 7.5 to 11.5 **(A),** and from 7.0 to 2.0 **(B)**.

Figure 4: ATPase activity concentration curve (90 min) of CAMKIV. Position of Pi and ATP spots are indicated.

Figure 5: The Discovery Studio 4.0 generated plots showing (A) the change of relative folding energy and (B) total charges with the increase in pH.

Figure 6 (A) The plot describing the variations in the RMSD values in the pH range 2.0-12.0 on the basis of 20 ns MD simulations. (B) The *R*g curves showing the variations in the structural compactness of the CAMKIV at different pH values.

Figure 7: The RMSF curve showing fluctuations of the constituent residues at different pH values during 20 ns MD simulations.

Table 1: Structural information of CAMKIV obtained from CD spectra at different pH values.

S .No	Buffers with different pH	α-helix	β-sheet	Random coil	θ_{222} mdeg cm^2 $dmol^{-1}$
1	GlyHCl pH, 2.0	4%	49%	47%	-6410
2	GlyHCl pH, 2.5	5%	48%	48%	-217
3	GlyHCl pH, 3.0	34%	14%	51%	-9284
4	Acetate pH,4.0	5%	48%	48%	-375
5	Acetate pH,5.5	31%	11%	59%	-9104
6	Cacodylate pH, 6.0	29%	11%	59%	-9110
7	Cacodylate pH, 6.5	28%	18%	54%	-9649
8	Cacodylate pH 7.0	26%	14%	60%	-9636
9	Mess pH, 6.0	31%	11%	58%	-9314
10	Mess pH, 6.5	31%	15%	53%	-8934
11	Mess pH,7.0	31%	14%	55%	-9144
12	Tris pH,7.5	30%	16%	54%	-8646
13	Tris pH,8.0	29%	20%	51%	-8679
14	Tris pH, 8.5	30%	16%	54%	-8881
15	Tris pH, 9.0	29%	24%	47%	-8762
16	Phosphate pH, 8.0	29%	23%	49%	-8990
17	Phosphate pH, 8.5	28%	16%	56%	-8768
18	Phosphate pH, 9.0	29%	21%	50%	-9035

19	Carbonate pH, 9.0	31%	11%	58%	-7982
20	Carbonate pH, 9.5	30%	16%	54%	-8432
21	Carbonate pH, 10.0	28%	21%	51%	-8929
22	GlyNaOH pH,10.0	27%	21%	52%	-8709
23	GlyNaOH pH,10.5	28%	31%	42%	-8696
24	GlyNaOH pH, 11.0	28%	23%	49%	-9042
25	GlyNaOH pH,11.5	29%	21%	49%	-9174

Figure 1

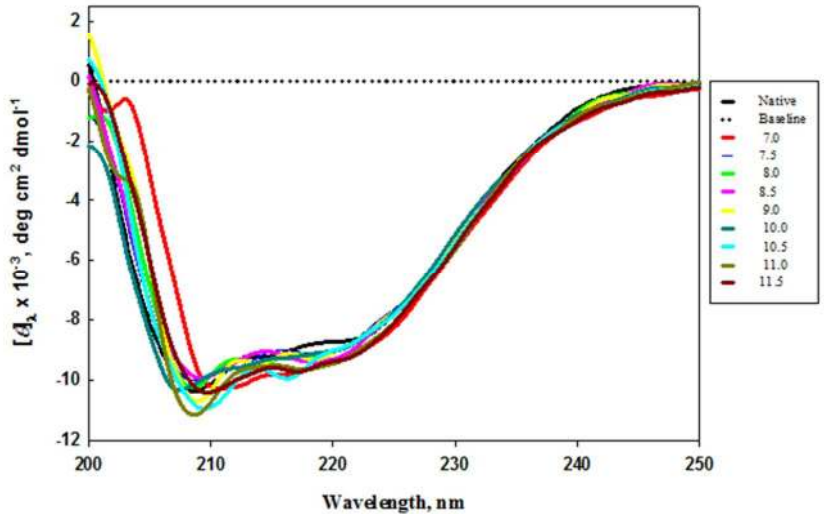

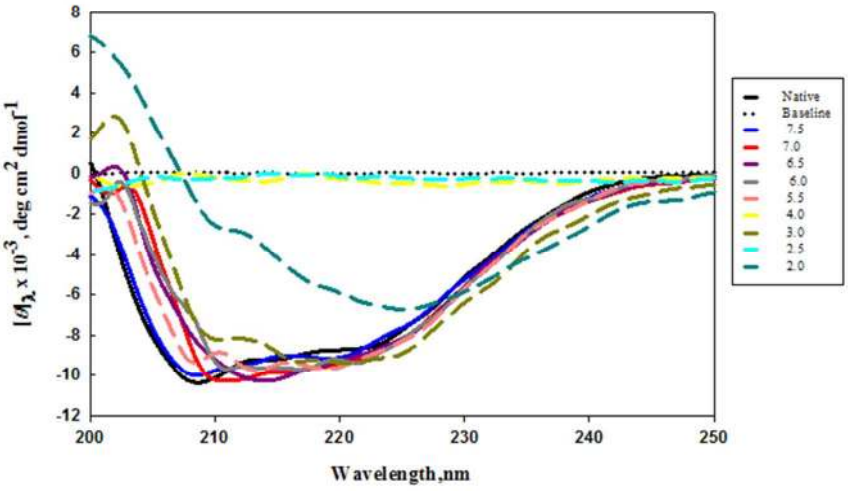

54x74mm (300 x 300 DPI)

Figure 2

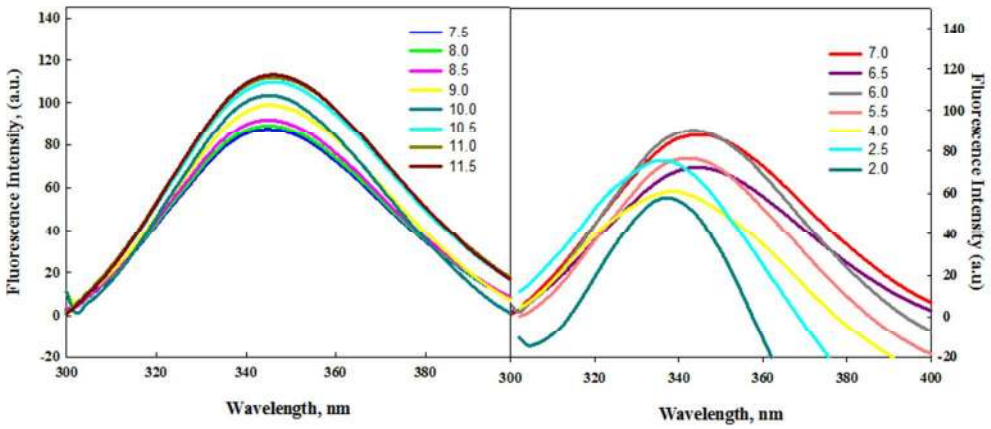

76x37mm (300 x 300 DPI)

Figure 3

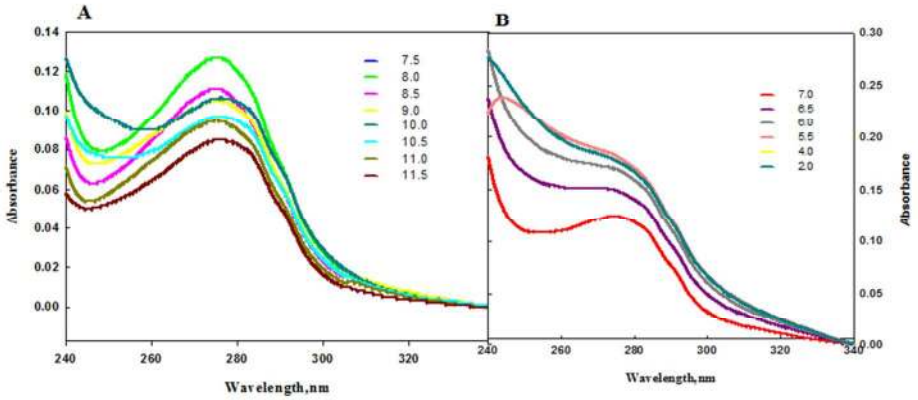

76x37mm (300 x 300 DPI)

Figure 4

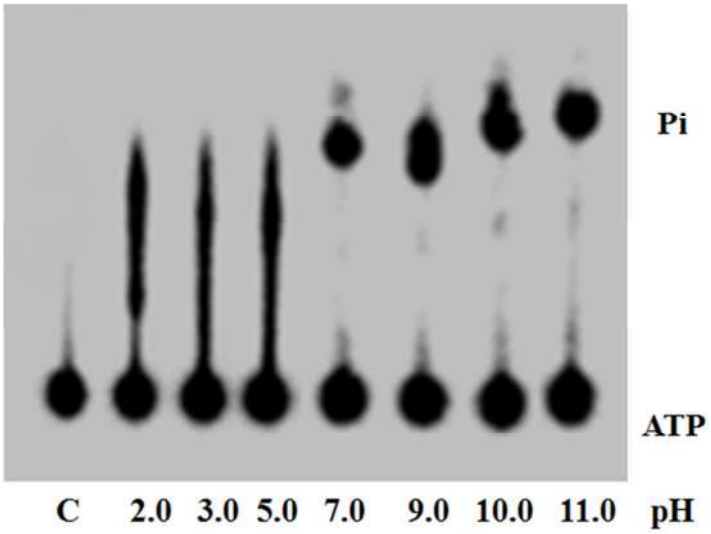

60x38mm (300 x 300 DPI)

Figure 5

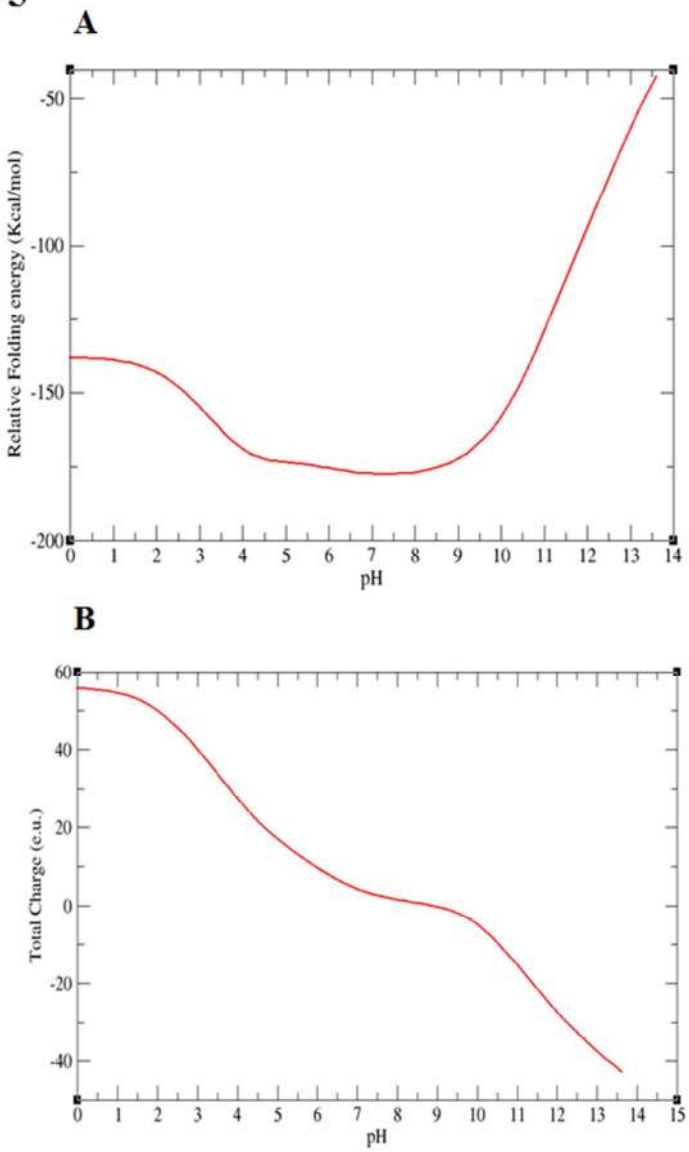

51x72mm (300 x 300 DPI)

Figure 6

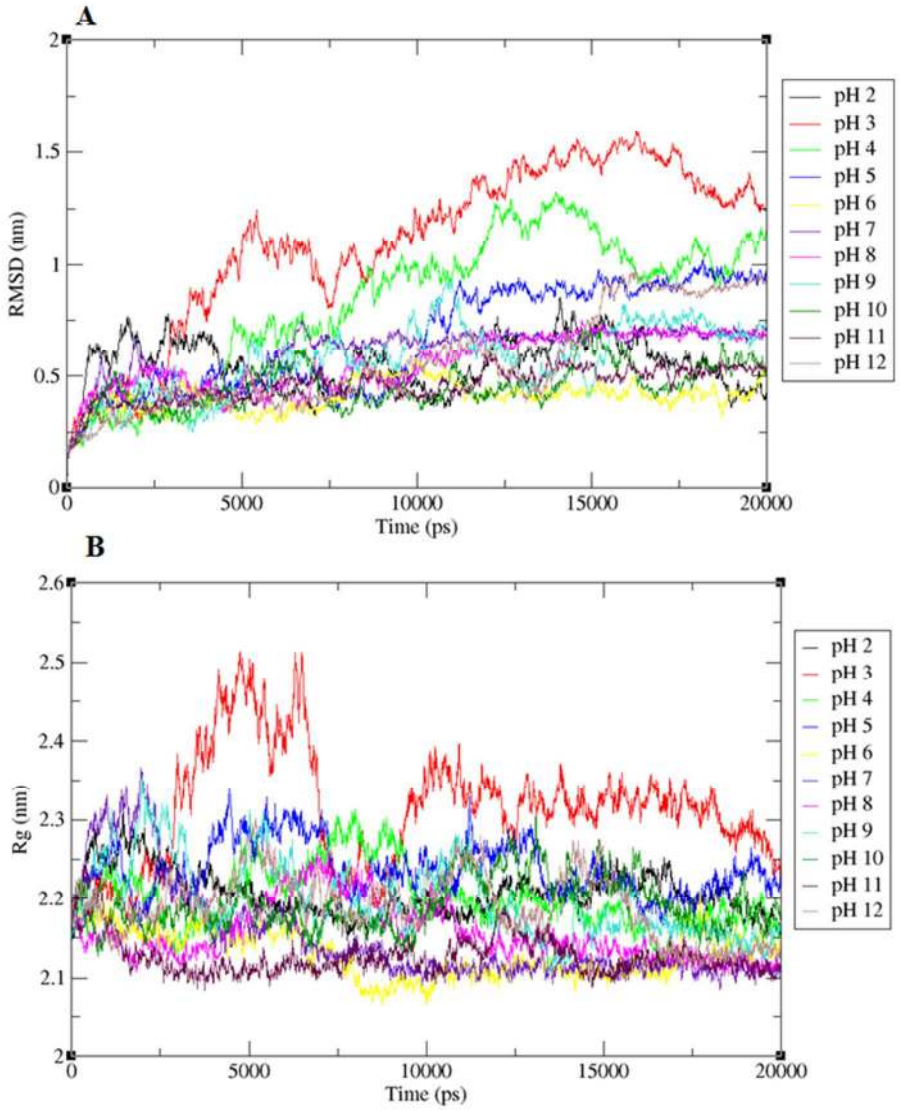

63x81mm (300 x 300 DPI)

Figure 7

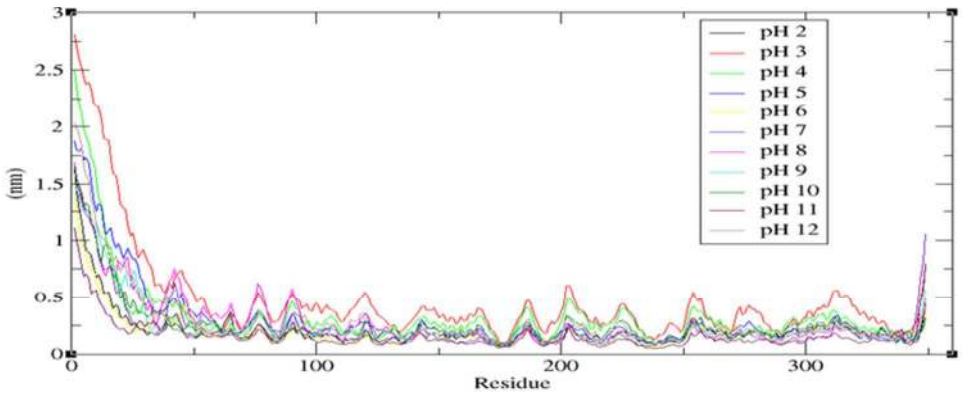

69x33mm (300 x 300 DPI)